JOURNAL OF OPTOELECTRONICS AND ADVANCED MATERIALS Vol. 10, No. 6, June 2008, p. 1511 - 1514

Short communication

Nonlinear dynamics of an optical injection VCSEL

ZHENGMAO WU[a*], GUANGQIONG XIA[a], HUIJUN KONG[a, b]
[a]*School of Physics, Southwest University, Chongqing 400715, China*
[b]*Electronic & Communication Engineering Department, Henan Mechanical and Electrical Engineering College, Xinxiang 453002, China*

In this paper, after taking into account two situations that the polarization of the injection light is parallel or orthogonal with the solitary vertical-cavity surface-emitting laser (VCSEL) output light, the nonlinear dynamic characteristics of an optical injection VCSEL are investigated numerically. The simulated results show that VCSEL can exhibit periodic oscillations, deterministic chaos and other complex instabilities under optical injection. For parallel or orthogonal optical injection, the same injection coefficients have different effects on the output of VCSEL. By properly adjusting the injection strength or detuning frequency, the dynamical state of the laser output can be controlled to a fixed state, and the polarization of the VCSEL output light can also be controlled.

(Received April 10, 2008; accepted June 4, 2008)

Keywords: Nonlinear dynamics, Vertical-cavity surface-emitting laser (VCSEL), Optical injection, Chaos

1. Introduction

External optical injection technique is widely used to reduce noise, enhance the bandwidth of modulation, and improve coherence property of semiconductor lasers [1-3]. Meantime, this technique has been proven to be an effective method to study the nonlinear dynamics of the semiconductor laser. However, the past relevant researches against this theme are mostly about edge-emitting lasers (EEL) [4-6] and relatively little about the vertical-cavity surface-emitting lasers (VCSELs). The VCSELs have many desirable characteristics such as low threshold current, single-longitudinal-mode operation and circular output-beam profile etc, and therefore have wide applications in optical interconnect, optical communication and many other relevant fields [7-9]. In order to examine the properties of VCSELs, efforts have been done to understanding the response of the VCSELs subject to optical injection by Torre *et al.* [10] and Li *et al.* [11]. Generally, typical VCSELs emit two perpendicular linear polarized lights along two crystallographic directions due to the weak cavity birefringence [12-15], which makes the nonlinear dynamics of optical injection VCSELs more complicated. Therefore, a deep understanding of the nonlinear dynamics of VCSEL subject to external optical injection is necessary. In this paper, the nonlinear dynamic characteristics of a VCSEL subject to polarization-preserved and polarization-rotated optical injection are studied numerically. The bifurcation diagrams of output intensity are investigated in detail, and the differences of nonlinear dynamic characteristics of VCSEL output between parallel and orthogonal optical injection are compared and analyzed systemically.

2. Theory

Fig. 1 shows the schematic setup of master (M-LD)-slave (S-VCSEL) configuration under consideration. A half-wave plat (HWP1) and a polarizing beam splitter (PBS) are used to adjust the injected intensity. The polarization of the injection light is controlled by HWP2. Optical isolator is used to avoid mutual injection.

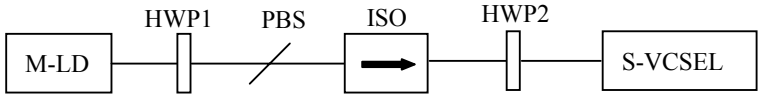

Fig. 1. Schematic of external optical injection VCSEL system.

The nonlinear dynamic characteristics of optical injection VCSEL have been studied assuming that the VCSEL supports two orthogonally polarized fundamental transverse modes, i.e. X-mode and Y-mode. Based on Lang-Kobayashi equations, the rate equations of the S-VCSEL can be expressed as

$$\frac{dE_x}{dt} = \frac{1}{2}(G_x - \gamma_x)E_x + k_x E_{inj}\cos\theta_x(t) \tag{1}$$

$$\frac{d\varphi_x}{dt} = \frac{\alpha}{2}(G_x - \gamma_x) - k_x \frac{E_{inj}}{E_x(t)}\sin\theta_x(t) \tag{2}$$

$$\frac{dE_y}{dt} = \frac{1}{2}(G_y - \gamma_y)E_y + k_y E_{inj}\cos\theta_y(t) \tag{3}$$

$$\frac{d\varphi_y}{dt} = \frac{\alpha}{2}(G_y - \gamma_y) - k_y \frac{E_{inj}}{E_y(t)}\sin\theta_y(t) \tag{4}$$

$$\frac{dN}{dt} = J - \frac{N}{\tau_s} - G_x\left|E_x(t)\right|^2 - G_y\left|E_y(t)\right|^2 \tag{5}$$

where the subscript x and y denote X-mode and Y-mode, respectively, E is the slowly varying amplitude of the slave VCSEL, E_{inj} is the slowly varying amplitude of the injection light, φ is the slowly varying phase, N is the carrier density, α is known as the linewidth enhancement factor, k is the injection coefficient, τ_s is the carrier lifetime, $\gamma=1/\tau$ is the reciprocal of the photo lifetime, J is the injection current density, and $\theta_{x,y}(t)= \varphi_{x,y}(t)-\Delta\omega_{ms}(t)$ ($\Delta\omega_{ms}$ is angular frequency detuning between the injection light and the emitted light of the solitary VCSEL), G is the gain and can be given by

$$G_{x,y} = \frac{g_{x,y}(N - N_0)}{1 + \varepsilon\left|E_{x,y}\right|^2} \tag{6}$$

where N_0 is the carrier density at transparency, ε is the nonlinear gain coefficient, and g is gain coefficient.

The differential equations above can be solved using fourth-order Runge-Kutta algorithm with the following coefficients: $N_0=1.3\times10^{24}m^{-3}$, $g_x=1.2\times10^{-12}$ m^3s^{-1}, $g_y=1.195\times10^{-12}$ m^3s^{-1}, $\alpha=5$, $\gamma_x=\gamma_y= 0.5\times10^{12}s^{-1}$, $\tau_s =2\times10^{-9}s$, $\varepsilon=0.5\times10^{-23}$, $J=1.05J_{th}$ (J_{th} is the threshold current density).

3. Results and discussion

The dynamic states of VCSEL subject to external optical injection vary with the change of the detuning frequency and injection coefficient. However, the same injection coefficients have different effects on the output of VCSEL under parallel or orthogonal optical injection. The nonlinear dynamic characteristics of VCSEL will be analyzed and discussed as follows.

3.1. X-polarization injection

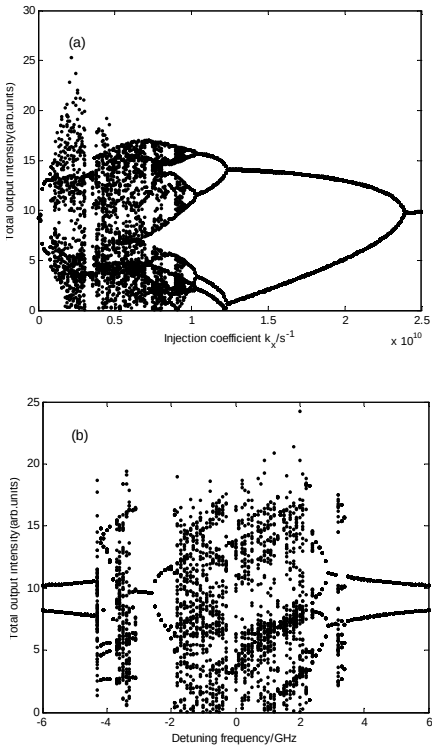

Fig. 2. *Bifurcation diagrams of total output intensity vs. injection coefficient k_x (a): $\Delta\omega_{ms}$ =0, and vs. detuning frequency $\Delta\omega_{ms}$ (b): $k_x=3.6\times10^9 s^{-1}$.*

For the case of X-mode injection (k_y=0), the injection light interacts directly with the lasing X-mode of the slave laser. Fig. 2 shows the bifurcation diagrams of total output intensity vs. injection coefficient k_x (fig. a) and vs. detuning frequency $\Delta\omega_{ms}$ (fig. b). With the increase of injection intensity, the laser exhibits period-one, period-two, multi-period, chaotic oscillation, multi-period, period-two, period-one and stable injection locking, as shown in fig. 2(a). With the change of the detuning frequency (see fig. 2(b)), the laser also exhibits various nonlinear dynamics and the bifurcation diagram is asymmetry against the center ($\Delta\omega_{ms}$ =0).

3.2. Y-polarization injection

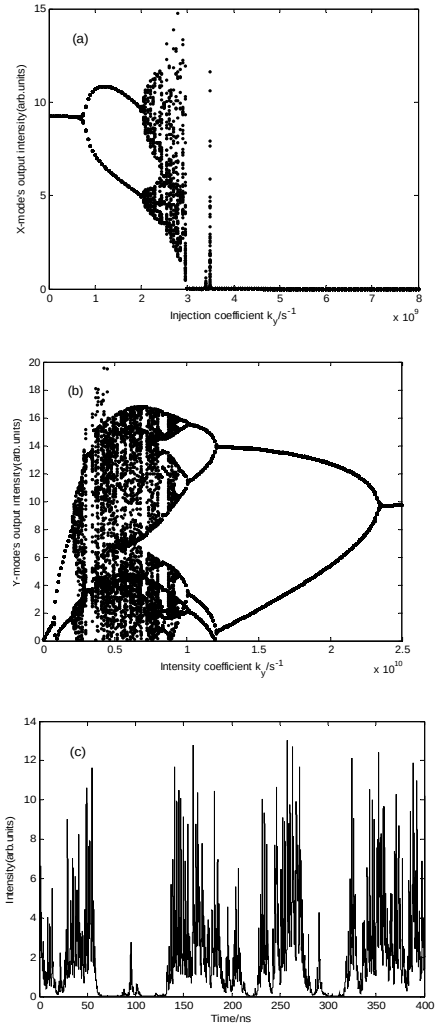

Fig. 3. Bifurcation diagrams of X-mode's output intensity (a) and Y-mode's output intensity (b) vs injection coefficient k_y at $\Delta\omega_{ms}$ = 0, and time series of X-mode output at $\Delta\omega_{ms}$ =0 and $k_y=3.5\times10^9 s^{-1}$.

Through rotating the HWP2, the polarization of the injection light can be adjusted to parallel with the suppressed Y- mode of the slave laser. In this case, the injection coefficient of X-mode is zero (k_x=0). The bifurcation diagrams of output intensity of X-mode and Y-mode are shown respectively in fig. 3 (a) and (b). With the increase of injection coefficient k_y, the output of the X-mode and Y-mode both become more and more instability and gradually evolve into chaotic state experiencing period-doubling process. When the injection coefficient is increased to 2.95×10^9 s^{-1}, X-mode is suppressed and the total output concentrates on Y-mode. However, X-mode lases again as the injection coefficient k_y is further increased to 3.5×10^9 s^{-1}. The reason may be that extremely complicated chaotic light emission occurs in the Y-mode, which induces a sufficiently large perturbation in the VCSEL to allow emission in the X-mode. The time series of X-mode is shown in fig. 3(c). To further increase the injection coefficient k_y , X-mode will be suppressed again. Finally, the output of the S-VCSEL is stably locked at Y-mode. Hence, the polarization of VCSEL can be controlled through adjusting the strength of the external optical injection.

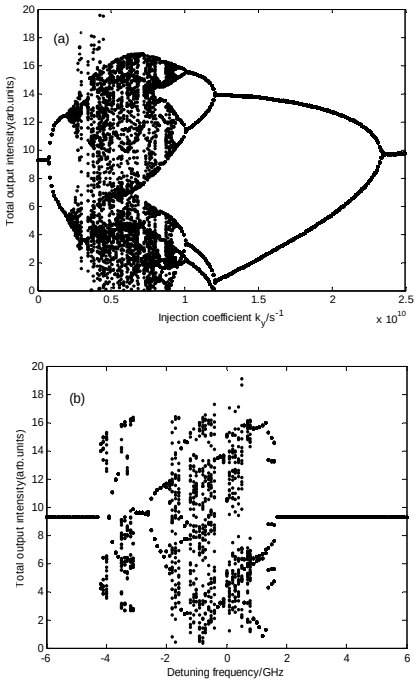

Fig. 4. Bifurcation diagrams of total output intensity vs. injection coefficient k_y (a): $\Delta\omega_{ms}$ =0, and vs. detuning frequency (b): $k_y=3.6\times10^9 s^{-1}$

The bifurcation diagrams of total output intensity vs. injection coefficient k_y and vs. detuning frequency $\Delta\omega_{ms}$ are plotted as shown in fig. 4. Comparing fig. 2(a) with fig. 4(a), it can be observed that under X-mode injection, the output of VCSEL evolves into chaotic state quickly with the increase of injection coefficient. However, under the Y-mode injection, the output of VCSEL evolves into chaotic state slowly and undergoes comparatively longer stable state and period-one oscillation. With the injection coefficient being further increased, the differences of nonlinear dynamics of VCSEL between parallel and orthogonal injection become more and more unobvious. Comparing fig. 2(b) with fig. 4(b), for a small detuning frequency, the difference of nonlinear dynamics of VCSEL between parallel and orthogonal injection is unobvious. With the increase of the detuning frequency, the differences become more and more obvious, especially at positive detuning frequency part. It can be concluded that under parallel or orthogonal optical injection, the same injection coefficients have different effects on the

output characteristics of VCSEL, and the differences become more and more obvious with the increase of the detuning frequency or the decrease of the injection coefficients. It is the interplay between the injection light and the optical field in the laser cavity that forms the overall basis for various nonlinear dynamic behaviors in an optical injection VCSEL [11, 16]. When the injection coefficient is relatively small or the detuning frequency is relatively large, the effect of the external injection light is comparatively weak, the difference between X-mode and Y-mode is determined mostly by the gain deficit, then the dynamic characteristics of X-mode and Y-mode are different significant. With the increase of the injection coefficient or decreasing the detuning frequency, the influence of the external injection light will be in an advantageous position, so the difference of nonlinear dynamics between X-mode and Y-mode becomes unobvious.

4. Conclusions

We have studied numerically the nonlinear dynamic characteristics of an optical injection VCSEL. With the injection coefficient and detuning frequency changed, the VCSEL exhibits various nonlinear dynamic behaviors, such as period-one oscillations, period-doubling and deterministic chaos. Under parallel or orthogonal optical injection, the same injection coefficients have different effects on the output of VCSEL, and the difference becomes more and more obvious with the increase of the detuning frequency or the decrease of the injection coefficient. By properly adjusting the injection strength or detuning frequency, the dynamical state of the laser output can be controlled to a fixed state, and the polarization of the VCSEL output light can also be controlled.

Acknowledgements

The authors acknowledge the support by Natural Science Foundation Project of CQ CSTC of the People's Republic of China, and the High-Tech Nurtured Fund of the Southwest University of the People's Republic of China.

References

[1] T. B, Simpson, J. M. Liu, A. Gavrielides, IEEE Photon. Technol. Lett. **7**, 709 (1995).
[2] J. M, Liu, H. F. Chen, X. J. Meng, T. B. Simpson, IEEE Photon. Technol. Lett. **9**, 1325 (1997)
[3] T. Chattopadhyay, M. Bhattacharya, IEEE/OSA J. Lightwave. Technol. **20**, 502 (2002).
[4] T. B. Simpson, J. M. Liu, A. Gavrielides, V. Kovanis, P. M, Phys. Rev. A **51**, 4181 (1995).
[5] S. Wieczorek, T. B. Simpson, B. Krauskopf, D. Lenstra, Opt. Commun. **215**, 125 (2003).
[6] H. J. Kong, Z. M. Wu, J. G. Wu, X. D. Lin, Y. K. Xie, G. Q. Xia, Chaos, Solitons & Fractals **36**, 18 (2008).
[7] K. Takaoka, M. Ishikawa, G. Hatakoshi, IEEE J. Sel. Top. Quantum Electron. **7**, 381 (2001).
[8] C. J. Chang-Hasnain, IEEE Commun. Mag. **41**, 530 (2003).
[9] R. Ju, P. S. Spencer, K. A. Shore, IEEE J. Quantum Electron. **41**, 1461 (2005).
[10] M. S. Torre, C. Masoller, K. A. Shore, IEEE J. Quantum. Electron. **40**, 25 (2004).
[11] X. F. Li, W. Pan, B. Luo, D. Ma, Y. Wang, N. H. Li, Chaos, Solitons & Fractals **27**, 1387 (2006).
[12] M. San-Miguel, Q. Feng, J. V. Moloney, Phys. Rev. A **52**, 1728 (1995).
[13] A. Vall, K. A. Shore, J. Sarma, IEEE J. Quantum Electron. **31**, 1423 (1995).
[14] S. F. Yu, IEEE J. Quantum Electron. **39**, 1362 (2003).
[15] D. Burak, J. V. Moloney, R. Binder, Phys. Rev. A **61**, 053809 (2000).
[16] T. B. Simpson, Opt. Commun. **215**, 135 (2003).

*Corresponding author: zmwu@swu.edu.cn